Measured electron energy distribution functions in inverted hydrogen fireballs

J. Gruenwald[1,2], J. Reynvaan[1]

[1] *Karl-Franzens Universität Graz, Institut für Physik, Universitätsplatz 5, 8010 Graz, Austria*
[2] *Gruenwald Laboratories GmbH, Taxberg 50, 5660 Taxenbach, Austria*

(Received: 20. Nov. 2025, Accepted: 22. Jan. 2026, Published online: 26. Jan. 2026)

Electron energy distribution functions (EEDFs) play an important role in many different types of plasmas. Their shape characterises the degree of thermal equilibrium, while the EEDF mean value is proportional to the electron temperature, if the distribution function is Maxwellian. In this paper we present the first measurements of EEDFs of electrons inside and outside an inverted fireball (IFB) plasma. It turns out that the EEDF inside the IFB plasma shows larger contributions from hot electrons, while on the outside there are two distinguished electron populations, namely cold bulk electrons and hot tail electrons. The measurements were carried out at low pressure of around 5 Pa, which is typical for IFB experiments. The measurements were performed with a movable Langmuir probe system, and the obtained I-V curves were used to calculate the EEDF. The measurements indicate a spread in the EEDF inside the IFB as well as a shift to higher peak values of the electron temperature. It was shown that there are basically two populations of electrons. There are the bulk electrons, which are relatively cold and a smaller number of hot electrons in the tail of the EEDF. Particularly, the electrons close to the wall of the IFB anode show a significantly broader EEDF, which indicates that they deviate from a Maxwellian distribution function and deviate, thus, from thermal equilibrium.

DOI: 10.31281/651j1c57

jgruenwald@g-labs.eu

I. Introduction

The knowledge of electron energy distribution function (EEDF) is fundamental in plasma physics because it directly influences key plasma parameters such as ionization rates, chemical reaction pathways, and energy transfer processes. By characterizing the EEDF, the behaviour of the plasma can be predicted and discharge conditions can be optimized for specific applications—ranging from materials processing and thin-film deposition to fusion research and plasma medicine. Furthermore, deviations from Maxwellian distributions, as revealed by EEDF measurements, provide critical insights into non-equilibrium effects and the underlying mechanisms governing electron kinetics in complex plasmas. A convenient way of determining the EEDFs is the second derivative of Langmuir probe curves. It is a standard technique in plasma physics and has been applied in various plasmas, ranging from low pressure discharges [1-5] to fusion plasmas [6,7]. If the EEDF can be considered isotropic, Druyvesteyn's method [8] can be applied [9]. This method is based on the determination of the EEDF via the second derivative of the I-V curve of a smoothed Langmuir probe trace. However, other authors have demonstrated that this evaluation technique is also reliable, even in the case of plasmas that are slightly anisotropic [10], as long as the pressure stays low (i.e., < 500 Pa) [11]. This is definitely the case in unmagnetized inverted fireball (IFB) experiments, where the typical

pressure ranges between 1 mPa [12,13] to several Pa in technologically relevant IFBs [14-24].

Knowledge of the EEDF allows insights into the kinetic behaviour of electrons in the plasma. Although the most important plasma parameters have been measured in IFB plasmas under various conditions, to the best of our knowledge, there are no data available for the EEDFs. Hydrogen was chosen for this work because it is an important working gas in many different industrial processes. On the other hand, it is the simplest molecular gas. Thus, the measurement of the EEDFs with a Langmuir probe system is expected to be straightforward and reliable. The EEDFs also help in understanding basic chemical mechanisms within the plasma. One example of such a mechanism is the reaction rate, which is calculated based on the EEDF [25]. Furthermore, EEDFs are also an indicator of the number of electron species (i.e., 'hot' and 'cold' electrons) in the plasma. The existence of these populations can be readily seen from the number of peaks of the distribution function. Monoenergetic electron populations lead to a single peak in the EEDF, while super-thermal electrons become visible in a second, smaller peak on the high-energy tail of the distribution function.

II. Measured EEDFs

All experiments in this work were carried out in a stainless steel plasma chamber that is specifically designed for IFB experiments and described in more detail elsewhere [26]. A schematic image of the setup is shown in Fig. 1:

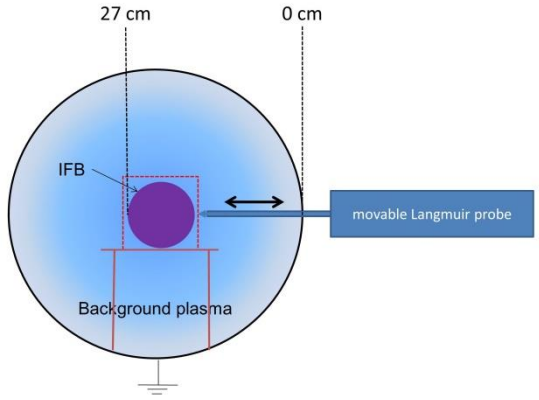

Figure 1: Schematics of the experimental setup with a movable Langmuir probe system.

The IFB cage electrode is a cylinder with 15 cm diameter, which was manufactured of a stainless steel mesh with 90 microns grid spacing and 20 microns wire thickness. The positions of the cage walls are located at 14.5 and 27.5 cm, respectively.

A moveable Langmuir probe system from Hiden Analytics was used for obtaining the I-V curves in hydrogen plasma. It has to be noted that electric probe measurements are commonly used due to their simplicity. However, they have the drawback that they are not non-invasive. To mitigate this disadvantage, the probe should always be as small as possible and have a simple geometrical shape. Normally, cylindrical, spherical or flat Langmuir probes are used. The probe tip in this work was a tungsten wire with 0.15 mm diameter and 10 mm length. The voltage range for the probe measurements was set from -70 V to + 100 V with respect to ground. The I-V curves were taken with 0.07 V increments over the entire voltage range. The working gas was H_2 5.0 at a constant pressure of 5 Pa. The primary plasma source for the IFB experiments was a tungsten filament with 7 cm length and 0.3 mm diameter. This filament was heated to 2650 K and a voltage difference of 137.6 volts was applied between the filament and the IFB cage electrode. The distance between the filament and the IFB anode was 50 cm. This distance ensures that the primary electrons from the filament can collide several times with neutrals before reaching the IFB cage. This creates a suitable background plasma for IFB experiments in the pressure range between 0.1 and 10 Pa.

Within this setup, a radial scan was performed, with I-V curves taken every cm. However, for the sake of readability, only the data for 4 cm intervals are shown in this work. These exemplary Langmuir probe curves are depicted in the following Fig. 2.

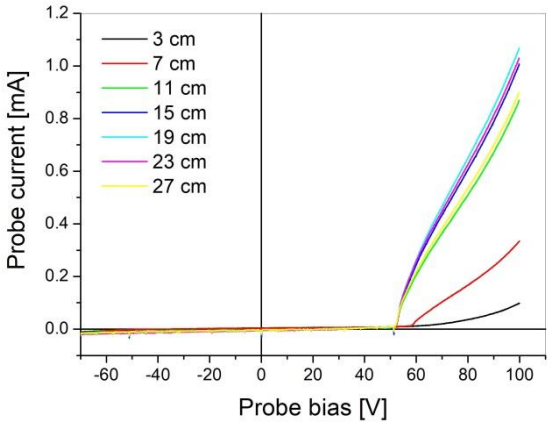

Figure 2: Exemplary I-V curves obtained through a radial scan inside and outside the IFB in hydrogen at 5 Pa.

The measurements were performed starting from the chamber wall moving inwards. A hole of 15 mm diameter was cut into one side of the IFB cage, to allow the entrance of the Langmuir probe. However, it was decided to leave the opposite wall of the IFB cage untouched to minimize the disturbance of the IFB plasma. As a consequence, the measurements were stopped at 27 cm, which is only a few mm away from the IFB cage back wall. It is also to be noted that the electron saturation currents in Fig. 2 are the highest at the positions 15, 19 and 23 cm, which are located inside the IFB. This means that the plasma density is substantially raised in this area. Outside the IFB (3, 7 and 11 cm from the chamber wall) the electron currents are much lower in comparison.

Following Druyvesteyn's method, the EEDF can be calculated from the second derivative of a Langmuir probe curve according to:

$$EEDF = \frac{2}{A_{pr}e^2}\sqrt{\frac{2eV}{m_e}}\frac{d^2I_{el}}{dV^2} \qquad (1)$$

Here, A_{pr} denotes the area of the Langmuir probe (4.73 mm² in our case), e is the elementary charge, m_e is the mass of the electron, I_{el} is the electron current of the probe and V is the corresponding probe voltage. For obtaining the EEDF, a linear fit was made to the ion current part of the probe curves. The fit function was then subtracted from the total probe current. Without the ion current considered, the remaining current of the probe trace is the pure electron current. This remaining electron current was smoothed with a Savitzky-Golay filter with an interpolation window width of n=191 and a polynomial degree of M=6. These parameters were chosen, because they have been proven to yield the smallest error when interpolating Langmuir probe curves [27].

The resulting normalized EEDFs are depicted in Fig. 3. It can be seen that most of the distribution functions are quite narrow and centred at around 2 eV, which is a typical value in low-pressure plasmas. However, towards the back side of the IFB grid, namely at 27 cm the EEDFs become broader, which indicates a deviation from the Maxwellian case. It is also notable, that in all positions, except the one at 27 cm, there is a hot tail population of the electrons. Particularly, at 23 cm, which is close to the centre of the IFB, the electron energy is up to 11 eV, while the electrons outside of the IFB electrode have only energies of about 9 eV. This is important because the hot tail electrons are the main driver of electron impact ionisation. The presence of electrons with 11 eV mean energy near the IFB centre is an indication of an increase in ionisation processes and, hence, plasma density. This is in agreement with findings in other works, like Refs. [15,18,19].

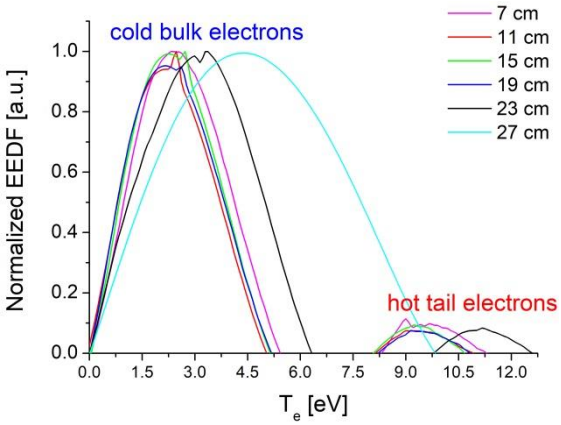

Figure 3: EEDFs calculated from the Langmuir probe traces depicted in Fig. 2.

In addition to the influence of electric fields from the anode wall, the broadening of the EEDF inside the IFB plasma is also a sign of increased energy exchange between the two populations. However, a high collisionality between the two species would lead to fast thermalisation, and, thus, to a single, well-defined EEDF. Normally, the electron collision mean free path in IFB experiments is in the order of the anode size. Hence, a full thermalisation of both electron populations is very unlikely. A more probable explanation is the occurrence of many inelastic collisions between the fast electrons and other particles. Dissociation and excitation events do not contribute directly to the shape of the EEDF. Hence, the EEDF broadening is attributed to ionisation events, which produce secondary electrons with rather small kinetic energy. At the same time the primary (ionizing) electrons loose considerable energy during a ionisation process. This shifts their position within the EEDF from the high-energy tail to lower values. The fact that there is a significant number of ionisation events is also reflected in the electron saturation current of the Langmuir probes (Fig. 2). One can see that the electron saturation current increases about tenfold inside the IFB plasma, compared to the probe curves taken outside the IFB anode. This also shows that the current continuity doesn't hold due to the efficient ionisation within the IFB. If current continuity would be fulfilled, the peak of the EEDF would shift to smaller values, which is clearly not the case.

In summary, the broadening of the EEDF close to the inside wall of the IFB anode indicates efficient

ionisation and a deviation from thermal equilibrium. However, the EEDF towards the centre of the IFB (at 23 cm) narrows again down and forms a Maxwellian distribution with electron temperatures of about 3 eV and a hot tail with an electron temperature around 11 eV.

III. Conclusion

The measured EEDFs reflect some important properties of IFBs, namely, the high plasma density around the core of the IFB and the presence of hot electrons in the tail of the EEDF, which are responsible for efficient electron impact ionisation inside the IFB anode. The narrow, well defined shape of the EEDFs indicate Maxwellian electron population, except at the close vicinity to the anode wall, where the EEDF peak is 'smeared out' and likely significantly disturbed by the strong electric fields from the IFB grid. Another factor that broadens the EEDF close to the anode is the occurrence of ionisation events and the inelastic collisions that cause these events. Close to the IFB centre, the thermal equilibrium is again intact, which is attributed to the high number of electron collisions in the IFB centre. Also, the peak value of the EEDF close to the IFB centre is about 1 eV higher than outside the IFB but still 2 eV smaller than the value close to the anode wall. These findings indicate that the IFB plasma is in thermal equilibrium (except very close to the anode border) and exhibits slightly elevated electron temperatures and a smaller population of high-energy tail electrons. These results underscore the influence of localized electric fields and collisional processes in shaping the EEDF inside IFB plasma, paving the way for further optimization of IFB performance for fundamental research and in technical applications.

IV. References

[1] Cox, T. I., et al. "The use of Langmuir probes and optical emission spectroscopy to measure electron energy distribution functions in RF-generated argon plasmas." *J. Phys. D: Appl. Phys.* 20.7 (1987): 820. https://doi.org/10.1088/0022-3727/20/7/002

[2] Demidov, V. I., et al. "Probe measurements of electron energy distributions in a strongly magnetized low-pressure helium plasma." *Phys. Plasmas* 6.1 (1999): 350-358. https://doi.org/10.1063/1.873288

[3] Xu, L. F., et al. "Measurement of plasma electron energy distribution functions by Langmuir probe using a modified AC modulation method." *Meas. Sci. Technol.* 36.1 (2024): 015902. https://doi.org/10.1088/1361-6501/ad8a7e

[4] Jauberteau, J. L., and Jauberteau, I. "Determination of the electron energy distribution function in weakly ionized plasma by means of a Langmuir probe and numerical methods." *AIP Advances* 14.5 (2024). https://doi.org/10.1063/5.0204161

[5] Gruenwald, J., et al. "Comparison of measured and simulated electron energy distribution functions in low-pressure helium plasmas." *Plasma Sources Sci. Technol.* 22.1 (2013): 015023. https://doi.org/10.1088/0963-0252/22/1/015023

[6] Crowley, B., et al. "Measurement of the electron energy distribution function by a Langmuir probe in an ITER-like hydrogen negative ion source." *Nucl. Fusion* 46.6 (2006): S307. https://doi.org/10.1088/0029-5515/46/6/S11

[7] Ivanova, P., et al. "Determination of the plasma potential and the EEDF by Langmuir probes in the divertor region of COMPASS tokamak." *J. Phys.: Conference Series*. Vol. 768. No. 1. IOP Publishing, 2016. https://doi.org10.1088/1742-6596/768/1/012003/.

[8] Druyvesteyn, M. J. "Der Niedervoltbogen." *Zeitschrift für Physik* 64.11 (1930): 781-798. https://doi.org/10.1007/BF01773007

[9] Allen, J. E. "On the applicability of the Druyvesteyn method of measuring electron energy distributions." *J. Phys. D: Appl. Phys.* 11.3 (1978): L35. https://doi.org/10.1088/0022-3727/11/3/001

[10] Woods, R. Claude, and Isaac D. Sudit. "Theory of electron retardation by Langmuir probes in anisotropic plasmas." *Phys. Rev. E* 50.3 (1994): 2222. https://doi.org/10.1103/PhysRevE.50.2222

[11] Arslanbekov, R. R., N. A. Khromov, and A. A. Kudryavtsev. "Probe measurements of electron energy distribution function at intermediate and high pressures and in a magnetic field." *PSST* 3.4 (1994): 528. https://doi.org/10.1088/0963-0252/3/4/010

[12] Stenzel, R. L., et al. "Transit time instabilities in an inverted fireball. I. Basic properties." *Phys. Plasmas* 18.1 (2011). https://doi.org/10.1063/1.3533437

[13] Stenzel, R. L., et al. "Transit time instabilities in an inverted fireball. II. Mode jumping and nonlinearities." *Phys. Plasmas* 18.1 (2011). https://doi.org/10.1063/1.3533440

[14] Reynvaan, J., et al. "Multiple Fireballs in a Reactive H_2/CH_4 Plasma." *IEEE Trans. Plasma Sci.* 42.10 (2014): 2848-2849. https://doi.org/10.1109/TPS.2014.2301494

[15] Gruenwald, J., Reynvaan, J., & Knoll, P. (2014). Creation and characterization of inverted fireballs in H_2 plasma. *Phys. Scripta*, *2014* (T161), 014006. https://doi.org/10.1088/0031-8949/2014/T161/014006

[16] Mayer, M., et al. (2016). Diamond like carbon deposition by inverted fireballs. *Mater. Today: Proc.*, *3*, S184-S189. https://doi.org/10.1016/j.matpr.2016.02.031

[17] Knoll, P., et al. "PECVD of carbon by inverted fireballs: From sputtering, bias enhanced nucleation to deposition." *Diam. Rel. Mater.* 65 (2016): 96-104. https://doi.org/10.1016/j.diamond.2016.02.021

[18] Gruenwald, J., Reynvaan, J., & Geistlinger, P. (2018). Basic plasma parameters and physical properties of inverted He fireballs. *PSST*, *27*(1), 015008. https://doi.org/10.1088/1361-6595/aaa332

[19] Gruenwald, J., Reynvaan, J., & Geistlinger, P. (2020). Influence of inhomogeneous electrode biasing on the plasma parameters of inverted H_2 fireballs. *JTSP*, *1*(1), 1-4. https://doi.org/10.31281/pvdgvf67

[20] Gruenwald, J., et al. "Application and limitations of inverted fireballs in a magnetron sputter device." *Surf. Coat. Technol.* 422 (2021): 127510. https://doi.org/10.1016/j.surfcoat.2021.127510

[21] Eichenhofer, Gerhard, et al. "Measurement of inverted n-hexane fireball properties with a Multipole Resonance Probe." *JTSP* 3.1 (2022): 109-117. https://doi.org/10.31281/jtsp.v3i1.23

[22] Gruenwald, J. (2022). Derivation of a simple engineering equation for the minimum voltage of inverted fireball onset. *JTSP*, *3*(1), 118-122. https://doi.org/10.31281/jtsp.v3i1.26

[23] Gruenwald, J., et al. "Inverted fireball deposition of carbon films with extremely low surface roughness." *Carbon Letters* 33.1 (2023): 225-231. https://doi.org/10.1007/s42823-022-00424-9

[24] Fenker, M., et al. "Pioneering work for the implementation of the inverted fireball technology for more effective PVD magnetron sputtering." *Surf. Coat. Technol.* 505 (2025): 132119. https://doi.org/10.1016/j.surfcoat.2025.132119

[25] Sun, J., & Chen, Q. "Kinetic roles of vibrational excitation in RF plasma assisted methane pyrolysis." *J. Energy Chem.*, *39*, 188-197 (2019). https://doi.org/10.1016/j.jechem.2019.01.028

[26] Gruenwald, J., J. Reynvaan, and Knoll, P.. "A plasma reactor optimized for inverted fireball experiments." *Rev. Sci. Instr.* 96.12 (2025). https://doi.org/10.1063/5.0303039

[27] Magnus, F., & Gudmundsson, J. T. (2008). Digital smoothing of the Langmuir probe IV characteristic. *Rev. Sci. Instr.*, *79*(7). https://doi.org/10.1063/1.2956970